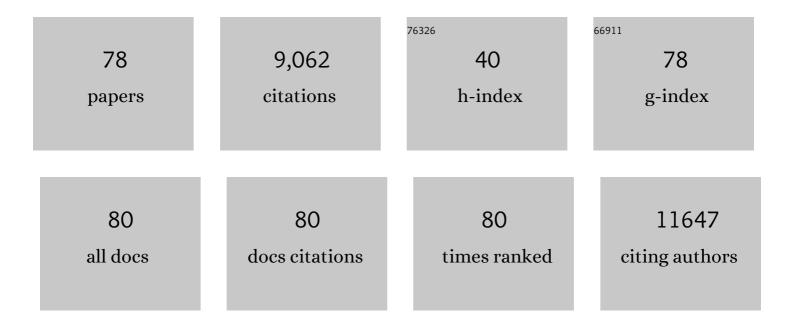
Shilei Xie

List of Publications by Year in descending order

Source: https://exaly.com/author-pdf/9257288/publications.pdf Version: 2024-02-01



Shilfi Xie

#	Article	IF	CITATIONS
1	Oxygen-deficient NiCo2O4 nanowires as the robust cathode for high-performance nickel–zinc batteries. Journal of Materials Research, 2022, 37, 2185-2194.	2.6	4
2	A Convenient Method for Synthesis of Fe ₃ O ₄ /FeS ₂ as High-Performance Electrocatalysts for Oxygen Evolution Reaction and Zinc-Air Batteries. Journal of the Electrochemical Society, 2021, 168, 030517.	2.9	4
3	Photoelectrochemical immunosensor based on CdSe@BiVO4 Co-sensitized TiO2 for carcinoembryonic antigen. Biosensors and Bioelectronics, 2020, 150, 111949.	10.1	44
4	Transparent PAN:TiO2 and PAN-co-PMA:TiO2 Nanofiber Composite Membranes with High Efficiency in Particulate Matter Pollutants Filtration. Nanoscale Research Letters, 2020, 15, 7.	5.7	21
5	Rational design of hybrid Fe7S8/Fe2N nanoparticles as effective and durable bifunctional electrocatalysts for rechargeable zinc-air batteries. Journal of Power Sources, 2020, 457, 228038.	7.8	20
6	Oxygen Functionalized CoP Nanowires as High-Efficient and Stable Electrocatalyst for Oxygen Evolution Reaction and Full Water Splitting. Journal of the Electrochemical Society, 2020, 167, 124512.	2.9	7
7	Comparative Proteomics Indicates That Redox Homeostasis Is Involved in High- and Low-Temperature Stress Tolerance in a Novel Wucai (Brassica campestris L.) Genotype. International Journal of Molecular Sciences, 2019, 20, 3760.	4.1	23
8	Transcriptome analysis reveals a positive effect of brassinosteroids on the photosynthetic capacity of wucai under low temperature. BMC Genomics, 2019, 20, 810.	2.8	29
9	Electrochemical Reduction of CO2 on Hollow Cubic Cu2O@Au Nanocomposites. Nanoscale Research Letters, 2019, 14, 63.	5.7	24
10	Theoretical studies on the purine radical induced purine–purine type intrastrand cross-links. Organic and Biomolecular Chemistry, 2019, 17, 892-897.	2.8	1
11	Functionalized N-Doped Carbon Nanotube Arrays: Novel Binder-Free Anodes for Sodium-Ion Batteries. ACS Applied Materials & Interfaces, 2019, 11, 18662-18670.	8.0	32
12	Comparative Proteomic Analysis Reveals That Chlorophyll Metabolism Contributes to Leaf Color Changes in Wucai (Brassica campestris L.) Responding to Cold Acclimation. Journal of Proteome Research, 2019, 18, 2478-2492.	3.7	17
13	A Sensor Based on Hollow, Octahedral, Cu 2 Oâ€Supported PalladiumÂNanoparticles – Prepared by a Galvanic Replacement Reaction – and Carboxylic Multiâ€Walled Carbon Nanotubes for Electrochemical Detection of Caffeic Acid in Red Wine. ChemistrySelect, 2019, 4, 4057-4063.	1.5	3
14	Comprehensive Evaluation for Cold Tolerance in Wucai (Brassica campestris L.) by the Performance Index on an Absorption Basis (Plabs). Agronomy, 2019, 9, 61.	3.0	18
15	Comparative Proteomics Reveals Cold Acclimation Machinery Through Enhanced Carbohydrate and Amino Acid Metabolism in Wucai (Brassica Campestris L.). Plants, 2019, 8, 474.	3.5	7
16	Voltammetric determination of levofloxacin using silver nanoparticles deposited on a thin nickel oxide porous film. Mikrochimica Acta, 2019, 186, 21.	5.0	21
17	A novel electrochemical ascorbic acid sensor based on branch-trunk Ag hierarchical nanostructures. Journal of Electroanalytical Chemistry, 2018, 818, 250-256.	3.8	35
18	Mechanism studies of addition reactions between the pyrimidine type radicals and their 3′/5′ neighboring deoxyguanosines. RSC Advances, 2018, 8, 2777-2785.	3.6	0

#	Article	IF	CITATIONS
19	Facile preparation of porous carbon nanomaterials for robust supercapacitors. Journal of Materials Research, 2018, 33, 1142-1154.	2.6	6
20	5-(Halomethyl)uridine derivatives as potential antitumor radiosensitizers: A DFT study. Chemical Physics Letters, 2018, 692, 374-381.	2.6	3
21	Three-dimensional structures of Mn doped CoP on flexible carbon cloth for effective oxygen evolution reaction. Journal of Materials Research, 2018, 33, 1258-1267.	2.6	20
22	Hierarchical MoS2@Polypyrrole core-shell microspheres with enhanced electrochemical performances for lithium storage. Electrochimica Acta, 2018, 269, 632-639.	5.2	34
23	Recent Advances toward Achieving Highâ€Performance Carbonâ€Fiber Materials for Supercapacitors. ChemElectroChem, 2018, 5, 571-582.	3.4	54
24	Oxygenâ€Vacancy and Surface Modulation of Ultrathin Nickel Cobaltite Nanosheets as a Highâ€Energy Cathode for Advanced Znâ€ion Batteries. Advanced Materials, 2018, 30, e1802396.	21.0	495
25	Ceria and ceria-based nanostructured materials for photoenergy applications. Nano Energy, 2017, 34, 313-337.	16.0	134
26	Enhanced Photoelectrochemical Activity by Autologous Cd/CdO/CdS Heterojunction Photoanodes with High Conductivity and Separation Efficiency. Chemistry - A European Journal, 2017, 23, 9625-9631.	3.3	14
27	DNA intrastrand cross-links induced by the purine-type deoxyguanosine-8-yl radical: a DFT study. Physical Chemistry Chemical Physics, 2017, 19, 16621-16628.	2.8	5
28	Advanced negative electrode of Fe 2 O 3 /graphene oxide paper for high energy supercapacitors. Materials Research Bulletin, 2017, 96, 413-418.	5.2	26
29	Nanoporous carbon derived from a functionalized metal–organic framework as a highly efficient oxygen reduction electrocatalyst. Nanoscale, 2017, 9, 862-868.	5.6	56
30	Formation of pyrimidine–pyrimidine type DNA intrastrand cross-links: a theoretical verification. Physical Chemistry Chemical Physics, 2017, 19, 28907-28916.	2.8	2
31	Binder-free WS ₂ nanosheets with enhanced crystallinity as a stable negative electrode for flexible asymmetric supercapacitors. Journal of Materials Chemistry A, 2017, 5, 21460-21466.	10.3	89
32	Non-enzymatic glucose biosensor based on palladium-copper oxide nanocomposites synthesized via galvanic replacement reaction. Sensors and Actuators B: Chemical, 2017, 253, 552-558.	7.8	25
33	Phase controllable synthesis of three-dimensional star-like MnO ₂ hierarchical architectures as highly efficient and stable oxygen reduction electrocatalysts. Journal of Materials Chemistry A, 2016, 4, 16462-16468.	10.3	48
34	Metal–Organicâ€Frameworkâ€Derived Dual Metal―and Nitrogenâ€Doped Carbon as Efficient and Robust Oxygen Reduction Reaction Catalysts for Microbial Fuel Cells. Advanced Science, 2016, 3, 1500265.	11.2	262
35	Chitosan Wasteâ€Derived Co and N Coâ€doped Carbon Electrocatalyst for Efficient Oxygen Reduction Reaction. ChemElectroChem, 2015, 2, 1806-1812.	3.4	49
36	Structural, Photocatalytic and Enhanced Magnetic Properties of Bi1-xHoxFeO3Nanoparticles Synthesized Via Sol-Gel Method. Ferroelectrics, 2015, 489, 65-72.	0.6	5

#	Article	IF	CITATIONS
37	Efficient and stable photoelctrochemical water oxidation by ZnO photoanode coupled with Eu2O3 as novel oxygen evolution catalyst. Journal of Power Sources, 2015, 297, 9-15.	7.8	25
38	Facile electrochemical synthesis of CeO ₂ hierarchical nanorods and nanowires with excellent photocatalytic activities. New Journal of Chemistry, 2014, 38, 2581-2586.	2.8	64
39	Oxygenâ€Deficient Hematite Nanorods as Highâ€Performance and Novel Negative Electrodes for Flexible Asymmetric Supercapacitors. Advanced Materials, 2014, 26, 3148-3155.	21.0	838
40	Gold nanoparticles inducing surface disorders of titanium dioxide photoanode for efficient water splitting. Nano Energy, 2014, 10, 313-321.	16.0	42
41	Heterostructured ZnO/SnO _{2â^'x} nanoparticles for efficient photocatalytic hydrogen production. Chemical Communications, 2014, 50, 4341-4343.	4.1	73
42	Photoelectrochemical hydrogen production from biomass derivatives and water. Chemical Society Reviews, 2014, 43, 7581-7593.	38.1	216
43	Remarkable photoelectrochemical performance of carbon dots sensitized TiO ₂ under visible light irradiation. Journal of Materials Chemistry A, 2014, 2, 16365-16368.	10.3	100
44	Oxygen vacancies enhancing capacitive properties of MnO2 nanorods for wearable asymmetric supercapacitors. Nano Energy, 2014, 8, 255-263.	16.0	381
45	Facile synthesis of tungsten oxide nanostructures for efficient photoelectrochemical water oxidation. Journal of Power Sources, 2014, 269, 98-103.	7.8	33
46	NiO decorated Mo:BiVO4 photoanode with enhanced visible-light photoelectrochemical activity. International Journal of Hydrogen Energy, 2014, 39, 4820-4827.	7.1	72
47	Improving the Cycling Stability of Metal–Nitride Supercapacitor Electrodes with a Thin Carbon Shell. Advanced Energy Materials, 2014, 4, 1300994.	19.5	217
48	Nickel Hydroxide Decorated Hydrogenated Zinc Oxide Nanorod Arrays with Enhanced Photoelectrochemical Performance. Electrochimica Acta, 2014, 137, 108-113.	5.2	29
49	Facile synthesis of large-area CeO 2 /ZnO nanotube arrays for enhanced photocatalytic hydrogen evolution. Journal of Power Sources, 2014, 247, 545-550.	7.8	60
50	Hydrogen production from solar driven glucose oxidation over Ni(OH)2 functionalized electroreduced-TiO2 nanowire arrays. Green Chemistry, 2013, 15, 2434.	9.0	72
51	Improving the photoelectrochemical and photocatalytic performance of CdO nanorods with CdS decoration. CrystEngComm, 2013, 15, 4212.	2.6	110
52	CdS/CeOx heterostructured nanowires for photocatalytic hydrogen production. Journal of Materials Chemistry A, 2013, 1, 4190.	10.3	61
53	Hierarchical CeO2 nanospheres as highly-efficient adsorbents for dye removal. New Journal of Chemistry, 2013, 37, 585.	2.8	62
54	Manganese dioxide nanorod arrays on carbon fabric for flexible solid-state supercapacitors. Journal of Power Sources, 2013, 239, 64-71.	7.8	121

#	Article	IF	CITATIONS
55	High Energy Density Asymmetric Quasi-Solid-State Supercapacitor Based on Porous Vanadium Nitride Nanowire Anode. Nano Letters, 2013, 13, 2628-2633.	9.1	691
56	3D MnO2–graphene composites with large areal capacitance for high-performance asymmetric supercapacitors. Nanoscale, 2013, 5, 6790.	5.6	258
57	TiO ₂ @C core–shell nanowires for high-performance and flexible solid-state supercapacitors. Journal of Materials Chemistry C, 2013, 1, 225-229.	5.5	192
58	Oxygen vacancies promoting photoelectrochemical performance of In2O3 nanocubes. Scientific Reports, 2013, 3, 1021.	3.3	427
59	Hâ€TiO ₂ @MnO ₂ //Hâ€TiO ₂ @C Core–Shell Nanowires for High Performance and Flexible Asymmetric Supercapacitors. Advanced Materials, 2013, 25, 267-272.	21.0	894
60	Enhanced photoactivity and stability of carbon and nitrogen co-treated ZnO nanorod arrays for photoelectrochemical water splitting. Journal of Materials Chemistry, 2012, 22, 14272.	6.7	85
61	Porous Pr(OH) ₃ Nanostructures as High-Efficiency Adsorbents for Dye Removal. Langmuir, 2012, 28, 11078-11085.	3.5	49
62	Stabilized TiN Nanowire Arrays for High-Performance and Flexible Supercapacitors. Nano Letters, 2012, 12, 5376-5381.	9.1	627
63	Controllable synthesis of hierarchical ZnO nanodisks for highly photocatalytic activity. CrystEngComm, 2012, 14, 1850.	2.6	75
64	Facile synthesis of porous 3D CoNiCu nano-network structure and their activity towards hydrogen evolution reaction. International Journal of Hydrogen Energy, 2012, 37, 18688-18693.	7.1	37
65	ZnO/SnO2 hierarchical and flower-like nanostructures: facile synthesis, formation mechanism, and optical and magnetic properties. CrystEngComm, 2012, 14, 2289.	2.6	36
66	Efficient photocatalytic hydrogen evolution over hydrogenated ZnO nanorod arrays. Chemical Communications, 2012, 48, 7717-7719.	4.1	253
67	Controllable synthesis of porous nickel–cobalt oxide nanosheets for supercapacitors. Journal of Materials Chemistry, 2012, 22, 13357.	6.7	207
68	Controllable Synthesis of Zn _{<i>x</i>} Cd _{1–<i>x</i>} S@ZnO Core–Shell Nanorods with Enhanced Photocatalytic Activity. Langmuir, 2012, 28, 10558-10564.	3.5	83
69	Facile preparation and photoelectrochemical properties of CdSe/TiO2 NTAs. Materials Research Bulletin, 2012, 47, 580-585.	5.2	26
70	Facile synthesis of Pr(OH)3 nanostructures and their application in water treatment. Materials Research Bulletin, 2012, 47, 1783-1786.	5.2	9
71	General electrochemical assembling to porous nanowires with high adaptability to water treatment. CrystEngComm, 2011, 13, 2451.	2.6	18
72	Monodisperse CeO2/CdS heterostructured spheres: one-pot synthesis and enhanced photocatalytic hydrogen activity. RSC Advances, 2011, 1, 1207.	3.6	80

#	Article	IF	CITATIONS
73	Controllable Electrochemical Synthesis and Photocatalytic Activity of CeO2 Octahedra and Nanotubes. Journal of the Electrochemical Society, 2011, 158, E41.	2.9	23
74	Redox cycles promoting photocatalytic hydrogen evolution of CeO2 nanorods. Journal of Materials Chemistry, 2011, 21, 5569.	6.7	120
75	Facile synthesis of large-area manganese oxide nanorod arrays as a high-performance electrochemical supercapacitor. Energy and Environmental Science, 2011, 4, 2915.	30.8	479
76	Vertically aligned In2O3 nanorods on FTO substrates for photoelectrochemical applications. Journal of Materials Chemistry, 2011, 21, 14685.	6.7	59
77	Facile Electrochemical Synthesis of ZnO/ZnS Heterostructure Nanorod Arrays. Journal of the Electrochemical Society, 2011, 158, E84.	2.9	13
78	Facile Electrochemical Synthesis of Single Crystalline CeO ₂ Octahedrons and Their Optical Properties. Langmuir, 2010, 26, 7569-7573.	3.5	107